Research Article

Performance Assessment of a Floating Photovoltaic Powerplant in Iran: A Case Study on Amir Kabir Dam, Karaj

Maryam Karami * , Mojtaba Azhdari Khameneh

Department of Mechanical Engineering, Faculty of Engineering, Kharazmi University, Tehran, Iran

ARTICLE INFO

ABSTRACT

In this study, a floating photovoltaic power plant (FPVPP) on the Amir Kabir dam in Karaj, Iran is designed and optimized in terms of energy, economic, and environmental analysis. The FPVPP is designed to supply the power needs of Varian village, which is located near the Amir Kabir dam. The results showed that under the same climatic conditions, the operating temperature of the panels of the ground-mounted PVPP is 4.7℃ higher than that of the floating PVPP, and the output voltage and power of the floating PVPP are 5.7 V and 2.05 kW higher than that of the ground-mounted one, respectively. The floating PVPP provides approximately 69.4% of the annual power needs of the Varian village. The average daily output of the floating PVPP is 280 kWh/day, which meets the daily needs of the village. The payback time is 9.88 years, 3.59 years, and 7.47 years by considering the electricity cost in Iran with subsidy and without subsidy and the electricity cost in the United States, respectively. The designed floating PVPP saves 488 m² of land and a total of about 260,000 m³ of water is directly and indirectly saved. This floating PVPP can prevent the emission of 22768 kg/year of carbon dioxide, 99 kg/year of sulfur dioxide, and 48 kg/year of nitrogen oxide.

1. Introduction

The significant increase in electricity demand, and excessive consumption of fossil fuels, along with environmental concerns around the world, imposes the installation of large-scale PVPP. However, the installation of PVPP needs land, which can have other strategic uses such as agriculture, animal husbandry, urban settlement, etc. To preserve the land and water, installing PVPPs on water bodies such as oceans, lakes, wetlands, reservoirs, irrigation ponds, sewage treatment plants, fish farms, dams, and canals can be an attractive alternative. Floating PVPPs have witnessed remarkable growth in recent years, driven by their numerous advantages over traditional ground-mounted PVPPs. These advantages include more efficient land use, higher efficiency, reduced water evaporation and environmental benefits.

By 2023, the global installed FPV capacity surpassed 2.5 gigawatts and is projected to reach 10 gigawatts by 2028. Several large FPV projects are underway or planned worldwide, including The 1.5-gigawatt Hyacinth project in Vietnam, The 400-megawatt Sungrow project in China, and The 200-megawatt Floating Solar Ranch project in California. Numerous smaller FPV projects are also in progress worldwide, demonstrating the growing interest in FPV as a sustainable and cost-effective renewable energy source. Iran has also made strides in FPV. The country's first FPV plant, with a 10-kilowatt capacity, was established in Isfahan Province in 2015. Since then, several other FPV projects have been commissioned in Iran, bringing the country's

---

total installed FPV capacity to over 1 megawatt. Given the numerous advantages of FPVs and the increasing interest in them, we can expect this industry to experience exponential growth in the coming years. FPVs have the potential to play a significant role in generating clean and sustainable energy worldwide [1].

The first floating PVPP was built in 2007 in Aichi, Japan. Between 2007 and 2014, other researchers developed their innovative floating PVPPs. The first commercial installation was a 175 kW PVPP, built at the Far Niente plant in California in 2008 [2]. In recent years, numerous studies on the floating PVPP have been conducted by the researchers. Rosa-Clot et al. [3] investigated the floating PVPP on Australian sewage ponds numerically and experimentally. The results showed that between 15,000 and 25,000 m^3 per MWp is saved in water consumption. The annual energy efficiency improves by up to 10% due to the better cooling effect. Widayat et al. [4] experimentally investigated the performance of monofacial and bifacial floating PVPP in a tropical area in Mahoni Lake, Jakarta, Indonesia. This study shows that the output energy delivered to the grid by the bifacial panel is 75.6% more than the monofacial one. Abd-Eljamid et al. [5] analyzed the experimental performance of the semi-submerged PVPP under weather conditions in Egypt. The obtained data indicated that the operating temperature decreased by 11.60%, the output power increased by about 20.28%, and the electrical efficiency increased by 49% at the wind speed of 32.82%.

Haas et al. [6] reported that the most optimal mode to cover the water surface is 40 to 60 percent. For moderate covers (40-60%), algal blooms are avoided due to reduced light in the reservoir without major economic losses of hydropower. Semeskandeh et al. [7] showed that the generation capacity and efficiency of FPVs are 19.47% and 27.98% higher than the ground-mounted one, respectively. Overall, the use of a floating PVPP reduces the payback time (PBT) to 6.3 years, which is 22.2% lower compared to a ground-mounted one. Pouran et al. [8] evaluated the environmental and technical impacts of a floating PVPP and found that they are well-matched with the existing HPP infrastructures, which support varying the energy supply and its flexibility.

Moraes et al. [9] studied the floating PVPP as an option for electricity supply in the Tocantins-Araguaia basin in Brazil, which depends on HPPs despite having problems with numerous droughts. Regarding the high solar energy potential of Brazil, floating PVPPs can be used to compensate for the lack of electricity. The results demonstrated the high potential of the floating PVPP to generate electricity ranging from 25.04 to 2555.04 TWh per year, and the range of 19.86 to 2024.30 million tons of carbon dioxide emissions avoided per year. A study of hydroelectric operations for hybridization by Pianco et al. [10] showed that the floating PVPP could produce 2 TWh more electricity than the HPP without significant change in the daily production of the HPP. This 50% increase is due to the volume available in the tank to store water during the day and use it during the night, which works as a free virtual battery for the floating PVPP. Ghigo et al [11] investigated a floating PVPP installed on an island in Italy to meet the island's electricity needs. The technoeconomic analysis by evaluating the main cost items of Capital expenditures, Operating expense, and levelized cost of energy (LCOE) indicated that although the obtained LCOE is significantly higher than a ground-mounted PVPP, the floating PVPP is competitive with other marine technologies, such as wind and offshore wave energy. Islam et al. [12] investigated the feasibility of using a floating PVPP in Bangladesh. The results showed that the optimal cost of energy for the floating PVPP is 0.0959 $/kWh, which is lower than the ground-mounted ones. In addition, the designed floating PVPP of 6.7 MW can supply 12.5% of local energy needs. Considering Türkiye's potential for floating PVPP by, Ateş [13] showed that the technical potential of the floating PVPP and the recycled water using the entire dams are 380,439 MW and 25.40 km^3 per year, respectively. By using only 10% of the dams' surface, the technical potential of the floating PVPP meets 39.67% of the total installed electricity capacity of Türkiye. The design and analysis of a floating PVPP with underground energy storage options for remote communities were investigated by Temiz and Dincer [14]. It was found that the proposed system with a 120 MW/s floating PVPP and energy storage options to meet all 51 GWh/year of non-thermal electrical provides 23.8 GWh/year of heating and 7.7 GWh/year of cooling loads for a community with 5320 people. Peng et al. [15] studied a new dynamic 2D fusion model and output characteristic analysis of floating photovoltaic modules considering motion and environmental factors. The results showed that the accuracy of the proposed model is more than 98.7%, and by using it, 2.5% can be added to the electricity generation efficiency of these systems. Results of the study done by Mumtaz et al. [16] on grid-connected mega-scale floatingPVPP showed that the Dam with cold in winter and hot in summer climatic conditions is a most feasible site with a (LCOE) of $0.047/kWh and a net present value (NPV) of million $1.7705, respectively. In contrast, a dam with mild cold climatic conditions

demonstrates the least feasible site with LCOE of $0.057/kWh and an NPV of million $1.0256, respectively. Chirwa et al. [17] research about FPVP in Zambia. The theoretical maximum potential was found to be 254.083 GWp, with the best option being 25.408 GWp at 10% coverage. The study aims to increase public awareness of floating solar photovoltaic systems and encourage investment in the technology. The findings could help alleviate Zambia's 0.81 GWp power deficit and promote the development of renewable energy sources like hydropower and solar photovoltaics. As a result of Mohammed Alsunousi and Erhan Kayabasi's [18] study, the carbon dioxide is captured in a carbon capture plant, and hydrogen is obtained from seawater in a hydrogen plant. The plant's efficiency is 0.21%, 0.5872%, and 0.1626%, with flue gas being the most important input parameter. The total cost for 30 years is $11.350 billion, with a production capacity of over 43.360 million tons of methanol. The plant is competitive with other clean synthetic fuel production plants. Moravej et al. [19] investigated the effect of SiO_2/water nanofluids on the electrical and thermal efficiency of domestic photovoltaic thermal systems (DPVT) theoretically and experimentally. The experimental results show that by increasing the concentration of nanofluid, the thermal and electrical performance is improved, and by increasing the diameter of nanoparticles, the overall efficiency is reduced. Balal et al. [20] focus on evaluating the effect of cooling on PV panel systems and its effect on electrical and thermal efficiency. The findings show that water cooling is more beneficial in terms of thermal energy production. In addition, this study shows that double-sided cooling, using jets to cool both sides of the PV panel, significantly increases the thermal and electrical efficiency, especially in hot and dry climates.

This research aims to design and analyze a grid-connected floating PVPP on the Amir Kabir dam in Karaj, Iran to supply the power needs of Varian village located near the dam. Based on the authors' knowledge, no studies have been conducted on this type of power plant for the Amir Kabir Dam. Due to drought and low water levels behind the dam, this method can be used to prevent excessive evaporation. Therefore, the objective of this study is also to investigate the reduction of water losses in the dam and increase the efficiency of PV panels using the cooling effect of water. The economic analysis and other environmental effects of the floating PVPP are also investigated.

2. Site Location

Figure 1 shows the site location of the designed floating PVPP. Amir Kabir Dam, also called Karaj Dam. It is the first multi-purpose dam in Iran, located on the Karaj River, 25 km north of Karaj city, at 35.97°N and 51.12°E. The dam area is 40 km², with an average annual water flow of 472 million m³. This area is mostly mountainous and includes valleys and mountains, and there is not enough space to install a PVPP; therefore, this dam was chosen to investigate power generation by a floating PVPP [21]. The height and length of the dam are about 180 m and 390 m, respectively. The total capacity of the dam reservoir is 202 million m³. The lower height of the reservoir and the natural water level of the reservoir are 1545 m and 1610 m, respectively. The HPP of Amir Kabir Dam has been connected to the national grid for more than 46 years [22].

The meteorological data of the considered site includes the annual average daily radiation at the horizon level of 5.51 kWh/m²/day, as well as the maximum daily temperature of 26.6℃ and the average wind speed equal to 3.69 m/s in the height of 10 m from the ground level. The elevation from the sea level of Varian village is 1788 m. Figure 2 shows the weather data for the site location. There are 23 families living in Varian village, and the average monthly electricity consumption for each family is 300 kWh. Considering the electricity consumption of other buildings in the village, such as the mosque, school, water pump, and health center, the monthly electricity consumption of this village is about 7100 kWh.

Fig. 1. Floating PVPP site location
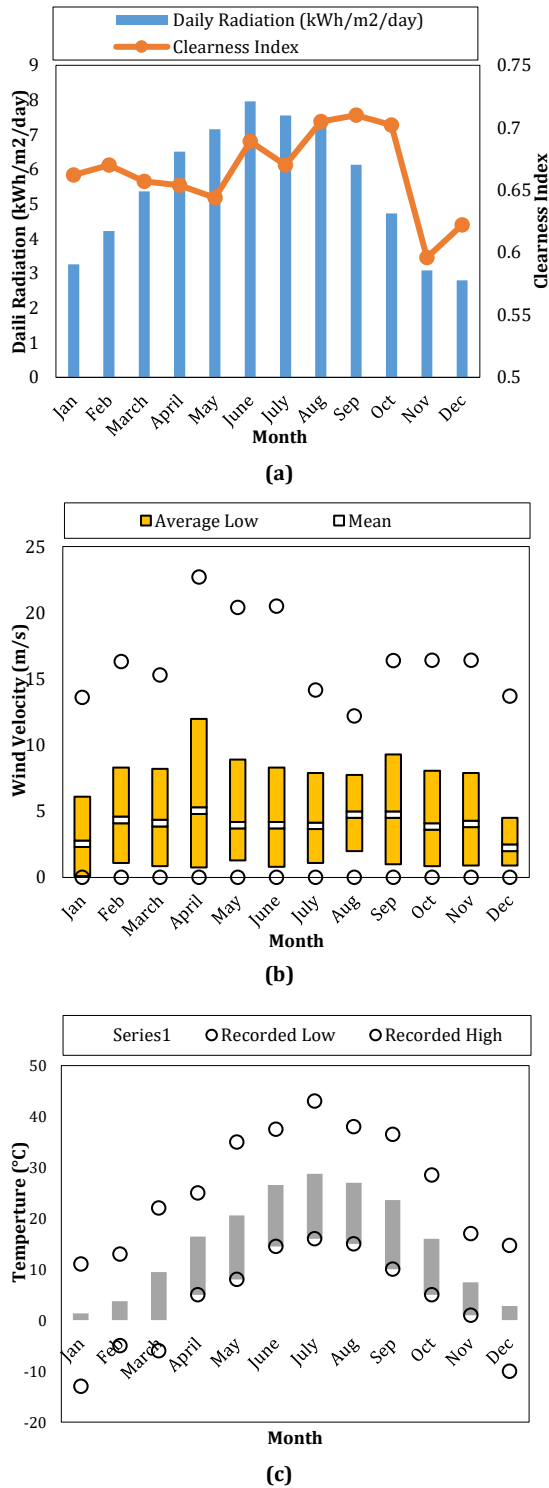
(a)

(b)

(c)

Fig. 2. Waether data for the site location (a) solar radiation, (b) wind velocity and (c) ambient temperature

3. Methodology

In this section, the floating PVPP is simulated in MATLAB/Simulink using the governing equations. Then, the economic analysis is done using Homer software. The environmental effects such as GHG emission, direct and indirect evaporation of water, and the land saving are stated.

3.1. Electrical Analysis

To design a grid-connected PVPP, the load supplied by the PVPP and grid must be determined. If the goal is to provide a part of the consumption load, the capacity of the PVPP should be designed in such a way that if the grid is interrupted, the PVPP can supply at least the important and necessary loads. In this study, the goal is to design a grid-connected PVPP that provides all required load.

A PV generator is mainly a set of solar cells, connectors, protective parts, and supports. Solar cells are made of semiconductor material, usually silicon, and are specially processed to form a positive electric field on one side (the back side) and a negative side, facing the sun, on the other. A solar cell is usually represented by an electrically equivalent diode model, as shown in Figure 3. This circuit can be used for a single cell, a module consisting of several cells, or an array consisting of several modules.
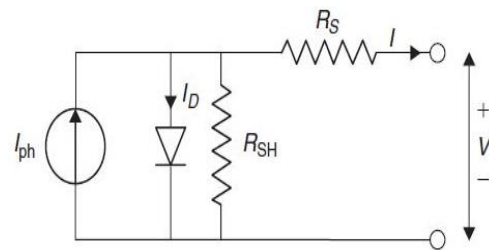

Fig. 3. Simple model of a solar cell [23]

According to Kirchhoff's law, the output current of the PV cell presented in Figure 3 is obtained by subtracting the diode current and the parallel resistor current from the current source. The characteristics of the output current-voltage of an ideal PV cell in the single-diode model are given in Eq. (1) [23]:

$$I = I_{ph} - I_o \left[\exp\left(\frac{V + R_s I}{V_t . A}\right) - 1 \right] - \frac{V + R_s I}{R_p} \tag{1}$$

where V_t is the thermal voltage [23]:

$$V_t = \frac{N_s a K T_{opt}}{q} \tag{2}$$

where I_o is diode saturation Current, q is the electron charge, K is Boltzmann constant, a is ideality factor of the solar cell, T_{opt} is operating temperature, N_s is the number of cells connected in series.

The mathematical model represented by Eq. (1) offers the best match with experimental values. By evaluating the five parameters I_{ph}, $R_s I$, I_o, a, and Rs, it is possible to model the PV module used in simulation and analysis accurately. These parameters are not directly given in the data sheets of commercial PV modules. I_{ph} can be evaluated by using the following equation [24]:

$$I_{ph} = [I_{sc} + K_{sc}(T - T_{ref})] \times G/1000 \qquad (3)$$

where, I_{sc} is current at short-circuit condition, K_{sc} is short-circuit current temperature coefficient, G is PV module illumination (W/m^2), T_{ref} reference temperature. Because I_{ph} is linearly proportional to the solar irradiance level, its value is scaled by this factor ($G/1000$) which is the ratio of the actual irradiance divided by the reference irradiance under STC. The temperature effect is reflected by the term $K_{sc} \Delta T$, which gives the variation in the photon current at an operating temperature. So, this term is added to the short-circuit current under STC. Eq.4 gives the total photon current generated under any weather conditions of solar irradiance and temperature [25].

It should be noted that I_{ph} is equivalent to a single PV cell's photon current. The two main differences between the diode characteristics are as follows: first, the voltage across the diode is increased by a factor of N_s, meaning that at open-circuit voltage, it is N_s times 0.6 V instead of being approximately 0.6 V. Secondly, the thermal voltage (V_t) of a single PV cell must also be scaled by the factor N_s. Since there are differences between the two resistances, the series resistance R_s for the entire module has a value equal to N_s times the series resistance of a single PV cell. In a similar vein, R_{sh} is the shunt of a single PV cell times N_s [25]. In this study, the PV panel chosen for the floating PVPP is AE SOLAR (AE665ME-132). The power of the selected panel is 665 W_p. The data sheet gives the currents and voltages at 3 salient operating conditions. They also sweep the terminal voltage from zero to open circuit and give the corresponding current versus voltage. This information together can be used to determine the various parameters such as $I_{ph}, R_s, I_{R_{sh}}$. The other diode characteristics can also be obtained from the information given in the data sheets. The first salient operating condition is the open-circuit condition so the opencircuit voltage V_{oc}, the current under which is equal to zero. The second salient operating condition is the short-circuit condition, so the corresponding short-circuit current I_{sc}, the voltage at which is equal to zero. The third salient condition is the maximum power point condition (MPP) at which the maximum of the voltage V_{mp} times the corresponding maximum current I_{mp} should be equal to the maximum power P_{max} of 665 watts.

At short-circuit condition and under standard test condition V=0 and $I = I_{sc}$. Eq. (1) becomes [25]:

$$I_{sc} = I_{ph} - I_o \left[\exp\left(\frac{I_{sc}R_s}{V_t}\right) - 1 \right] - \frac{I_{sc}R_s}{R_{sh}} \qquad (4)$$

The diode voltage $V_d = I_{sc}R_s$ is low and has a value similar to V_t for normal values of R_s, which are usually in the range of a few tenths of ohms. The entire term corresponding to the diode current Id is negligible for tiny values of Rs and short-circuit conditions because Io is in the nanoampere range. Similar to how the shunt current Ish is negligible given that R_{sh} is a few hundred ohms, the same rationale applies here since V_d or the voltage across the shunt resistance is very small. I_{sc} therefore simply equals Iph under short-circuit conditions, as determined by Eq. (4) [25]:

$$I_{sc} = I_{ph} \qquad (5)$$

Since I_{sc} is provided by the manufacturer at STC, I_{ph} is also estimated at STC. Then to get I_{ph} value under any arbitrary conditions other that the STC, one can use the expression under Eq. (3) [25]. The equations required to calculate the series resistance R_s and the shunt resistance R_{sh} may then be obtained by first estimating the slopes of the I-V curves under open-circuit and short-circuit conditions, respectively. The slope of the current varies greatly depending on the value of the shunt resistance since it mostly influences the I-V curve's slope during short-circuit conditions. The value of the slope decreases with increasing shunt resistance and vice versa. The series resistance has a major impact on the I-V curve's slope in the vicinity of the open-circuit condition. The I-V curve's slope at open circuit conditions falls as the series resistance continues to rise. As a result, this relationship may be used to calculate the series resistance based on the I-V curve's slope under open-circuit conditions.

$$\frac{dI}{dV} = -\frac{I_o}{V_t}\left(e^{\frac{V+IR_s}{V_t}}\left(1 + \frac{R_s dI}{dV}\right)\right)$$
$$-\frac{1}{R_{sh}} - \frac{R_s}{R_{sh}}\frac{dI}{dV} \qquad (6)$$

$$\frac{dI}{dV}\left(1 + \frac{R_s}{R_{sh}} + \frac{I_o R_s}{V_t} e^{\frac{V+IR_s}{V_t}}\right) =$$
$$-\frac{I_o}{V_t}\left(e^{\frac{V+IR_s}{V_t}}\right) - \frac{1}{R_{sh}} \qquad (7)$$

Under short-circuit condition,

$$I_o e^{\frac{V+IR_s}{V_t}} = I_o e^{\frac{I_{sc}R_s}{V_t}} \approx 0 , R_s \ll R_{sh}$$

$$R_{sh} = -\frac{dV}{dI} \mid at\ short - circuit\ condition \qquad (8)$$

On the other hand, the shunt resistance is simply the inverse of the slope of the I-V curve at short-circuit condition [26]. Under open-circuit condition [25]:

$$I_o e^{\frac{V+IR_s}{V_t}} = I_o e^{\frac{V_{oc}}{V_t}} = I_{sc} \tag{9}$$

Hence, Eq. 7 becomes:

$$\frac{dI}{dV}\left(1 + R_s\left(\frac{1}{R_{sh}} + \frac{I_{sc}}{V_t}\right)\right) = -\left(\frac{I_{sc}}{V_t} + \frac{1}{R_{sh}}\right) \tag{10}$$

$$\left(1 + R_s\left(\frac{1}{R_{sh}} + \frac{I_{sc}}{V_t}\right)\right) = -\frac{dV}{dI}\left(\frac{I_{sc}}{V_t} + \frac{1}{R_{sh}}\right) \tag{11}$$

$$R_s = -\frac{dV}{dI} - \frac{1}{\left(\frac{1}{R_{sh}} + \frac{I_{sc}}{V_t}\right)} \tag{12}$$

With $\frac{1}{R_{sh}} \ll \frac{I_{sc}}{V_t}$

$$R_s = -\frac{dV}{dI} - \frac{V_t}{I_{sc}} \tag{13}$$

Under open-circuit condition, $I = 0$ and $V = V_{oc}$. Combining eq. 1 and 5, one can get:

$$I_o\left(e^{\frac{V+IR_s}{V_t}} - 1\right) = I_o e^{\frac{V_{oc}}{V_t}} = I_{sc} - \frac{V_{oc}}{R_{sh}} \tag{14}$$

This Exponential term is extremely large compared to 1, in the order to 10^9 so one can get:

$$I_o = \frac{I_{sc} - \frac{V_{oc}}{R_{sh}}}{e^{\frac{V_{oc}}{V_t}}} \tag{15}$$

while R_{sh} has previously been determined using Eq.8, V_{oc} and I_{sc} are directly taken from the datasheet. Once more, the word V_t, which is provided by the expression containing the diode ideality factor a, is troublesome. This temperature-dependent factor has an experimental range of 1 to 2. A lower value indicates a superior diode semiconductor material, which lowers the saturation current I_o value [25].

By replacing voltage at maximum power V_{mp} and current at maximum power I_{mp} in the current equation under Eq. 2, one can leverage the fact that the ideality factor's impact is most pronounced close to the maximum power point MPP to estimate the ideality factor (a). At maximum power point, $V = V_{mp}$, $I = I_{mp}$

$$I_{mp} = I_{sc} - I_o\left(e^{\frac{V_d}{V_t}} - 1\right) - \left(\frac{V_d}{R_{sh}}\right) \tag{16}$$

where, $V_d = V_{mp} + I_{mp}R_s$.

For modeling a floating PVPP, the main factors that determine the cell temperature are wind speed and water temperature. As mentioned before, the difference between ground-mounted and floating PVPPs is the operating temperature. In the following, the mathematical modeling of these conditions is discussed [27]:

$$T_w = 5 + 0.75T_{amb} \tag{17}$$

where T_w is water temperature. The maximum annual ambient temperature (T_{amb}) is considered 26.625°C.

The wind speed on the water is higher than that on the ground:

$$V_{ws} = 1.62 + 1.17V_{wl} \tag{18}$$

where V_{ws} and V_{wl} are the wind speed on the water and ground, respectively.

The cell temperature on the water (T_{cw}) and on the gound (T_c) is calculated using the following relations [28]:

$$T_{cw} = 0.943T_w + 0.0195G$$
$$-1.528V_{ws} + 0.3529 \tag{19}$$

$$T_c = 0.943T_{amb} + 0.0195G$$
$$-1.528V_{wl} + 0.3529 \tag{20}$$

The required rated power of the PVPP is obtain as follow [29]:

$$P_{pvarray} = \frac{EE}{\left(\frac{G}{G_{STC}}\right)\left(f_{\frac{DC}{AC}}\right)f_{temp}} \cong 54\ Kw_p \tag{21}$$

where EE is Estimated Energy required per day(Wh/day), $f_{DC/Ac}$ is the DC to AC de-rating factor (%) from DC to AC, which is equal to 0.778 [27]:

$$f_{temp} = 1 - \beta(T_{cw} - T_{STC}) \tag{22}$$

where β is the reduction temperature coefficient, which is equal to 0.45%. As a result, the output power for the PV array is approximately equal to 54 peak kW (kWp); therefore, a PVPP with nominal power equal to this value should be designed.

The number of the required panels ($N_{panels} = \frac{P_{pvarray}}{P_{panel}}$) is equal to 82 [30]. Before determining the required number of strings and the number of panels of each string, it is necessary to define the DC/AC inverter for use in the PP. In this study, the Sunny Tripower 2500TL is selected, which is of the three-phase, string inverters type and is special for PPs connected to the grid The number of series panels ($NP_{strings} = \frac{V_{Max.inverte}}{V_{Max.panel}}$) and strings ($N_{strings} = \frac{N_{panels}}{NP_{string}}$) are obtained 16 and 6, respectively. Therefore, the total number of modified panels is equal to 96. Take into account that each inverter has 2 MPPs and that each MPP can have a maximum of 3 strings, it gives a maximum of 6 strings per inverter. To distribute all the 6 strings across the inverters, the final distribution needs 1 inverter [31].

The floating and ground-mounted PVPPs are simulated in MATLAB/Simulink software, which can be seen in Figure 4.

The only difference between floating and ground-mounted PVPPs is the temperature of the panels, and the other conditions are the same. The model inputs are the panel temperature on the water surface (Eq. (19)), and the solar radiation intensity according to weather data of the site location, which is 5510 W/m^2.

Table 1 shows other input data for simulation. According to the geographical coordinates of the site location (longitude 51.12°E and latitude 35.97°N), the annual optimal slope is considered 33.5°[32].

Table 1. Input data for simulation

Input Data	Symbol	Value
Temperature in STC	$T_{STC}(k)$	298.15
Open-circuit voltage	$V_{oc}(V)$	46.10
Intensity of solar radiation in STC	$G(W/m^2)$	1000
Temperature coefficient of short circuit current	$I_{oc}(\%/°C)$	0.004
Maximum power temperature coefficient	$P_{max}(\%/°C)$	-0.34
Short-circuit current In STC	$I_{sc}(A)$	18.49
Maximum of the voltage	$V_{mp}(V)$	38
Maximum current	$I_{mp}(A)$	17.5
Ideality factor	A	3.106
Panells in series	N_s	16
Panells in string	N_p	6
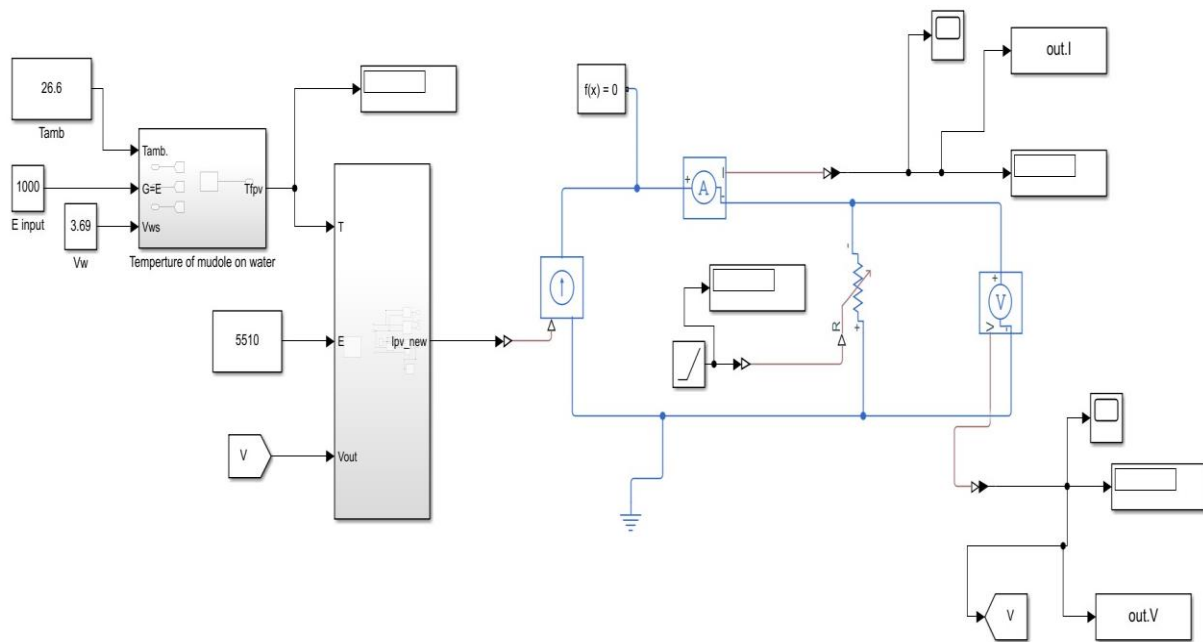
Fig. 4. Modeling of PVPP in MATLAB/Simulink

3.2. Economic Analysis

In this study, due to the low cost of energy in Iran, economic analysis is done for three cases of considering the electricity cost in Iran with (Case 1) and without subsidies (Case 2), as well as the electricity cost in the United States (Case 3). The details of purchasing and selling backing tariffs from/to the grid are seen in Table 2.

Table 2. Purcasing and sell backing tariffs from/to the grid

	Iran-with subsidy ($/kWh)	Iran-without subsidy ($/kWh)	US ($/kWh)
Power Price	0.004	0.14	0.19
Sellback Price	0.04	0.04	0.68

The cost and lifetime of a PV panel are $218 per kWp and 25 years, respectively; however, these PPs include pontoons, cables, support systems, workers' pay, etc., which must be added to the panel cost. Maintenance costs are usually assumed to be a percentage of the initial cost and are assumed to increase at a certain rate per year.

For fixed (non-tracking) floating PVPP, maintenance can be considered as 1% of the initial cost [23]. The selected inverter has a nominal DC power equal to 25550 W, a lifespan of 15 years, and an efficiency of 98.30, according to the product catalog. Table 3 shows the initial and operating costs of the panels and inverter. During the life of the PP, the inverter is replaced once. For the study of the economic conditions of Iran, a discount rate of 23%, an inflation rate of 46.50%, and a lifetime of 25 years were considered. An inflation rate of 4.05% and a discount rate of 5.25% were set for the United States.

Table 3. Initial and operating cost of panels and inverter

	Capacity (kW_p)	Capital ($)	Replacement ($)	Operating and Maintenance (O&M)
Generic flat plate PV				
Iran	54	33,000	14,220	330
USA	54	198,000	83,100	1,980
Inverter				
Iran	25.550	5,300	4,320	53
USA	25.550	3,200	3,150	32

3.3. Environmental Analysis

3.3.1. Evaporation Reduction

A floating PVPP covers a large area of the water surface, so the water resources are saved by reducing water evaporation losses. This is a direct effect of the water saving of the floating PVPP. When a floating PVPP is installed on a reservoir or a dam, the electricity generated can be used to replace the electricity generated by the HPP. This is the indirect effect of PVPP on water saving.

In this study, it is assumed that 1) evaporation is proportional to the exposed surface of the water body and 2) the rate of evaporation is uniform over the entire surface of the water body. Therefore, the direct effect on water saving can be calculated as the following:

$$E = E_0 \times C \times p \tag{23}$$

where E is the evaporation reduction due to the floating PVPP and E_0 is the evaporation loss without using the floating PVPP, which is 1.2-0.9 million m³/km² for the studied project. C is the surface area covered by the water, and p is the prevention coefficient assumed in the study to be 0.9.

The indirect water-saving effect is calculated by converting the electricity generated by the floating PVPP to the volume of water consumed by the HPP:

$$V_e = \frac{0.75 \times 3600 \times E_{PV,e} \times (1 - \epsilon)}{\rho \times g \times \Delta H} \tag{24}$$

where V_e is the volume of the water source. $E_{PV,e}$ is the power generation of the floating PVPP. ϵ is the discarding rate of PV power and H is the water head [33].

3.3.2. Land Saving

This study evaluates the effect of floating PVPP on land saving through the power density parameter, which measures the installed capacity of a floating PVPP per unit of water surface. Based on the average power density, the technical capacity and generation potential of water bodies (reservoir, lake, canal, etc.) are evaluated for the installation of a floating PVPP:

Technical capacity potential

$$= Urban\ open\ space \times\ Power\ Density \tag{25}$$

Technical production potential

$$= \sum [UO \times PD \times CF \times OH] \tag{26}$$

where, Uo is urban open space, PD is power density, CF is capacity factor, and OH is operating hours.

3.3.3. GHG Emission Reduction

The GHG emission reduction of a floating PVPP with the GHG produced from a fossil fuel PP at the same electricity generation is estimated:

$$G_t = E_s \times 10^{-3} \times G \times (1 + \beta) \qquad (27)$$

where G_t is the reduction of GHG emissions (tons of carbon dioxide/year), E_s is the electricity generated by the floating PVPP per year (MWh/year), G is the standard GHG emissions of each country (tons of carbon dioxide) /year), and β is the average loss rate of power transmission and distribution [34].

4. Results and Discussion

4.1. Comparison of Ground-Mounted and Floating PVPPs

In the designed PP, the output current from the panel enters an electrical circuit. The circuit includes a variable resistor that can calculate and measure the output voltage, current, and power of the panel. According to the product catalog (AE SOLAR (AE665ME-132)), the output voltage and current of the panel should be 46.10 V and 18.45 A under standard test conditions. The modeled panel produces a DC voltage of 46.06 V and a current of 18.49 A, which show the error of 0.086% and 0.2% compared to the product catalog, respectively.

Figure 5 shows the variation of PVPP outputs. As seen, the ground-mounted and floating PVPPs have an output voltage of 467.3 V and 473 V of DC electricity, which leads to the generation of 224.45 kW and 226.5 kW, respectively.
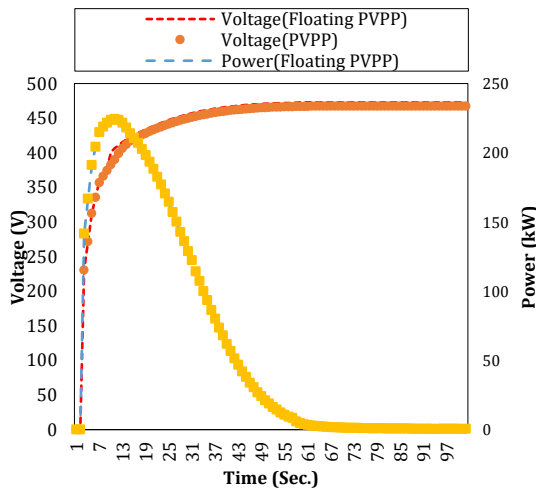

Fig. 5. Output voltage and power of ground-mounted and floating PVPP

Under the solar radiation of 5510 W/m² and the wind speed of 3.69 m/s, the center of the PV cell reaches its highest temperature of 38.25℃ in the ground-mounted PVPP and 33.55℃ in the floating one. The results indicate that the cooling effect of water causes a difference in the operating temperature of about 5℃ between the two PPs. Table 4 shows the comparison of the operating parameters of the PPs for the site location.

Table 4. Performance indicators of floating and ground-mounted PVPP

PVPP type	Output voltage (V)	Output power (kW)	Operating temperature (℃)
FPVPP	473	226.5	33.55
PVPP	467.3	224.5	38.25

4.2. Electrical Analysis

The monthly power supply by the floating PVPP and the grid is shown in Figure 6. It can be seen that most of the power demand is provided by the floating PVPP. The power generated by the floating PVPP from May to August is more than in other months due to the high intensity of solar radiation. As expected, the use of the grid increases in the months with the low power generation by the PVPP. The grid is used because of the lack of solar radiation at night or cloudy weather. During a year, the share of the required power supply by the floating PVPP is approximately 69.4%, and the share of the grid is 30.6%.
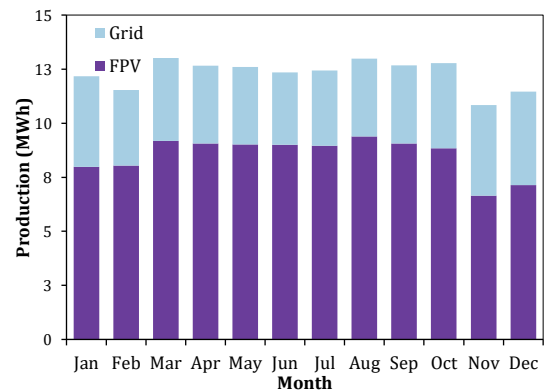

Fig. 6. Power supply by floating PVPP and grid

The PVPP working hours and days are shown in Figure 7. As seen, the PVPP works in almost half of the hours of the year, and its capacity factor, which is the ratio of energy generated over a time period (typically a year) divided by the installed capacity, is equal to 21.6%. Also, the average daily output of the floating PVPP is 280 kWh, which meets the village's need (237 kWh). The surplus of output is sold to the grid.
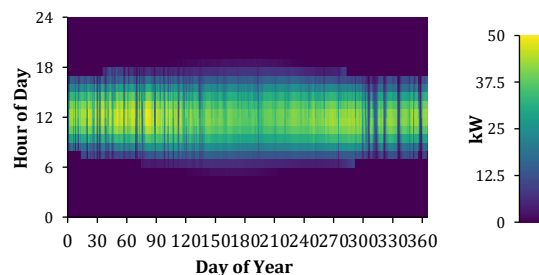

Fig. 7. Floating PVPP power output

Figure 8 (a) shows the different hours and days when the required power is supplied from the grid, which is mainly at night and on winter days, and Figure 8 (b) shows the sale of surplus power generated by the floating PVPP to the grid. It is found that the maximum power sold to the grid is in the middle of the day due to the high intensity of solar radiation. The annual energy purchased from the grid is 45,155 kWh, and the annual energy sold to the grid is 39,034 kWh. Table 5 shows the monthly purchased and sold energy of the designed power plant for the case study.
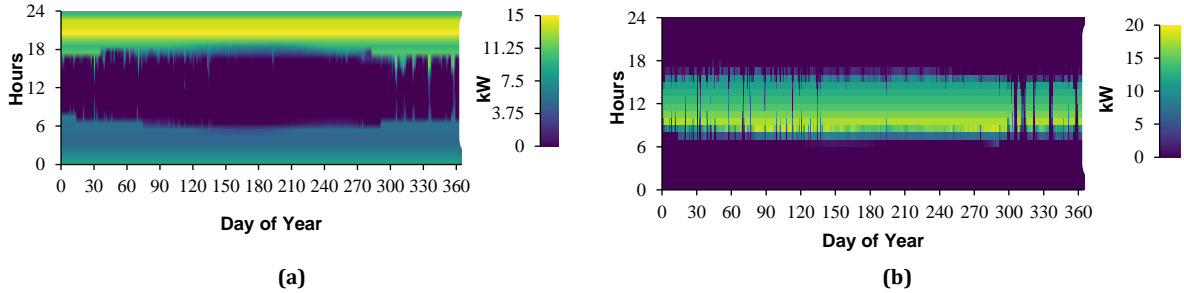

Fig. 8. Power (a) purchased and (b) sellbacked from/to the grid

Table 5. Monthly purchased and sellbacked power

Month	Purchased Power (kWh)	Sellbacked Power (kWh)	Net Power Purchased (kWh)	Peak Load (kW)	Power Charge
January	4,188	2,987	1,201	15.0	-$104.81
February	3,489	2,908	581	15.0	-$104.12
March	3,828	3,361	467	15.0	-$121.04
April	3,587	3,422	165	15.0	-$124.34
May	3,581	3,510	71.0	15.0	-$127.87
June	3,350	3,579	-229	15.0	-$131.43
July	3,478	3,586	-108	15.0	-$131.25
August	3,603	3,711	-108	15.0	-$135.82
September	3,610	3,498	111	15.0	-$127.30
October	3,932	3,453	479	15.0	-$124.34
November	4,181	2,407	1,774	15.0	-$81.66
December	4,329	2,612	1,717	15.0	-$89.34
Annual	45,155	39,034	6,121	15.0	-$1,403

4.3. Economic Analysis

For all the mentioned economic conditions (cost of electricity in Iran with and without subsidies, as well as the cost of electricity in the United States), the optimal economic PP is the floating PVPP connected to the power grid. Table 6 shows economic indicators for all cases. As can be seen, for this case, the PBT in Case 1 is in 9.88 years, and PBT does not happen for the simple payback (without considering the discounte rate). For Case 2, the PP is much more economical than Case 1, so the PBT occurs in 3.59 years, while the PBT for the simple payback is 5.50 years. According to Table 6, for the US economic conditions, the PBT occurs in 7.12 years, and also due to the low inflation rate, the PBT in the simple payback is very close to the PBT in the discounted case and is equal to 7.47 years. It is concluded from the results of the economic conditions that the PP is less economical than in the case where the subsidy is added to the electricity cost.

Table 6. Economic analysis results

Metric	Value		
	Case 1	Case 2	Case 3
Present worth ($)	$661,630	$3,410,00	$406,682
Annual worth ($/yr)	$1,358	$7,000	$19,000
Return on invesrment (%)	-0.8	13.9	10.5
Internal rate of return (%)	n/a	17.7	13.4
Simple payback (yr)	n/a	5.50	7.12
Discounted payback (yr)	9.88	3.59	7.47

4.4. Environmental Effect

In Table 7, the environmental effects of the floating PVPP are listed. As seen, the floating PVPP with a peak power of 54 kW needs a water level of 488 m² , which means saving 488 m² of land resources if the same capacity of PVPP is installed on land. This amount of water surface coverage covers only 0.0122% of the dam area, which creates minor effects on the reservoir and related activities such as tourism and fish farming. The direct water saving effect is calculated as avoided evaporation loss, and the proposed integrated HPP and floating PVPP can preserve the water supply of 19870 m³ per year. The indirect effect of water saving is calculated as saving water consumption for HPP. Considering the average Discarding rate of PV power of 13%, the indirect water saving corresponds to about 240,010 m³. In other words, the floating PVPP saves about 260,000 m³ of water from evaporation and consumption every year, which is the per capita water consumption of 3715 people per year. As can be seen in Table 7, by using the floating PVPP, the emission of environmental pollutants is almost halved.

Table 7. Environmental effect of floating PVPP

Parameter	Value
Dam area (km^2)	40
The area occupied by the power plant (km^2)	0.000488
Indirect water saving (m^3/yr)	240010
Direct water saving (m^3/yr)	19870
Reduction of carbon dioxide production ($kg/year$)	22768
Reducing sulfur dioxide production ($kg/year$)	98
Reduction of nitrogen oxide production ($kg/year$)	48

5. Conclusions

In this study, first, the 3E analysis of a floating PVPP on Amirkabir dam in Karaj, Iran, connected to the grid is performed and compared with a ground-mounted PVPPs. The results can be summarized as the following:

- In the climatic conditions of the average solar radiation of 5.51 kWh/m²/day, the average wind speed of 3.69 m/s, and the average ambient temperature of 25.5℃, the operating temperature of the panels of the ground-mounted PVPP was about 5℃ higher than that of the floating PVPP. The output voltage and power of the floating PVPP was 5.7 V and 2.05 kW more than that of the ground-mounted PVPP, respectively.

- The annual share of the required power supply from the floating PVPP is approximately 69.4%. The average daily output of the designed PVPP is 280 kWh/day, which meets the daily needs of the village, which is 237 kWh/day, and the excess generation (43 kWh/day) is sold to the grid. The floating PVPP generates the required power of almost half of the hours of the year (4386 hours).

- The economic evaluation of the floating PVPP was investigated for three cases considering the cost of electricity in Iran with and without subsidies, as well as the cost of electricity in the United States. The results showed that the floating PVPP connected to the grid was the optimum PVPP. The PBT was 9.88 years for electricity cost with subsidy, 3.59 years for electricity cost without subsidy, and 7.47 years for electricity cost in the United States.

- The designed floating PVPP saves 488 m² of land, especially for the studied area, which is mostly mountainous, and a total of about 260,000 m³ of water is directly and indirectly saved, which is the water consumption of 3715 people per year. This floating PVPP can prevent the emission of 22768 kg/year of carbon dioxide, 98 kg/year of sulfur dioxide and 48 kg/year of nitrogen oxide.

Nomenclature

A	Diode quality factor
C	Covered water surface area (m^2)
CF	Capacity factor
$E_{PV,e}$	Power generation of the floating PVPP (W)
ER	Estimated energy required (Wh/day)
E_0	Evaporation loss in natural conditions (kg)
$f_{DC/Ac}$	DC to AC de-rating factor (%)
FF	Fill factor
f_{temp}	Temperature factor
G	Global Irradiation (W/m^2)
G_m	Standard amount of greenhouse gas emissions (kg)

G_{STC}	Global Irradiation STC (W/m^2)
G_t	Reduction of greenhouse gas emissions (kg)
H	Water head (m)
I_o	Dark saturation current (A)
I_{oc}	Open circuit current (A)
I_{sc}	Short-circuit current (A)
I_{mp}	Maximum power point current (A)
I_{ph}	Photocurrent (A)
k	Boltzmann's gas constant
N_{panels}	Number of required Panels
$NP_{strings}$	Number of required panels in series
$N_{strings}$	Number of required panels in strings
N_s	Cells connected in series
OH	Operating Hours (hr)
p	Prevention coefficient
$P_{pvarray}$	Rated power of the power plant (kW_p)
PD	Power density
q	Electron charge
R_p	Parallel resistance of the shunt current panel (Ω)
R_s	Series resistance (Ω)
T_{amb}	Ambient temperature (℃)
T_c	Cell temperature on the ground (℃)
T_{cw}	Cell temperature on the water (℃)
T_{STC}	Temperature of Standard test condition (℃)
T_w	Water temperature (℃)
UO	Urban open space
V	Voltage imposed across the cell (V)
V_e	Volume of water source (V)
V_{oc}	Open circuit voltage (V)
V_{mp}	Maximum power point voltage (V)
V_{wl}	Land wind speed (m/s)
V_{ws}	Water wind speed (m/s)
V_t	Thermal voltage (V)

Greek symbols

ϵ	PV power dissipation rate
β	PV cell temperature in current time step (%)

Subscript

amb	Ambient
mpp	Maximum Power Point
OC	Open circuit
SC	Short-circuit
STC	Standard Test Condition
temp	Temperature

Conflicts of Interest

The author declares that there is no conflict of interest regarding the publication of this article.

Reference

[1] Aweid, R.S., Ahmed, O.K. and Algburi, S., 2024, March. Recent developments of floating photovoltaic power plants: A review. In AIP Conference Proceedings (Vol. 2885, No. 1). AIP Publishing.

[2] Yousuf, H., Khokhar, M.Q., Zahid, M.A., Kim, J., Kim, Y., Cho, E.C., Cho, Y.H. and Yi, J., 2020. A review on floating photovoltaic technology (FPVT). Current Photovoltaic Research, 8(3), pp.67-78.

[3] Rosa-Clot, M., Tina, G.M. and Nizetic, S., 2017. Floating photovoltaic plants and wastewater basins: an Australian project. Energy Procedia, 134, pp.664-674.

[4] Widayat, A.A., Ma'arif, S., Syahindra, K.D., Fauzi, A.F. and Setiawan, E.A., 2020, October. Comparison and optimization of floating bifacial and monofacial solar PV system in a tropical region. In *2020 9th international conference on power science and engineering (ICPSE)* (pp. 66-70). IEEE.

[5] Abd-Elhamid, H.F., Ahmed, A., Zeleňáková, M., Vranayová, Z. and Fathy, I., 2021. Reservoir management by reducing evaporation using floating photovoltaic system: A case study of Lake Nasser, Egypt. Water, 13(6), p.769.

[6] Haas, J., Khalighi, J., De La Fuente, A., Gerbersdorf, S.U., Nowak, W. and Chen, P.J., 2020. Floating photovoltaic plants: Ecological impacts versus hydropower operation flexibility. Energy Conversion and Management, 206, p.112414.

[7] Semeskandeh, S., Hojjat, M. and Hosseini Abardeh, M., 2022. Techno–economic–environmental comparison of floating photovoltaic plant with conventional solar photovoltaic plant in northern Iran. Clean Energy, 6(2), pp.353-361.

[8] Pouran, H.M., Lopes, M.P.C., Nogueira, T., Branco, D.A.C. and Sheng, Y., 2022. Environmental and technical impacts of floating photovoltaic plants as an emerging clean energy technology. IScience, 25(11).

[9] Moraes, C.A., Valadão, G.F., Renato, N.S., Botelho, D.F., de Oliveira, A.C., Aleman, C.C. and Cunha, F.F., 2022. Floating photovoltaic plants as an electricity supply option in the Tocantins-Araguaia basin. Renewable Energy, 193, pp.264-277.

[10] Piancó, F., Moraes, L., dos Prazeres, I., Lima, A.G.G., Bessa, J.G., Micheli, L., Fernández, E. and Almonacid, F., 2022. Hydroelectric operation for hybridization with a floating photovoltaic plant: A case of study. Renewable Energy, 201, pp.85-95.

[11] Ghigo, A., Faraggiana, E., Sirigu, M., Mattiazzo, G. and Bracco, G., 2022. Design and analysis of a floating photovoltaic system for offshore installation: The case study of Lampedusa. Energies, 15(23), p.8804.

[12] Islam, M.I., Maruf, M.H., Al Mansur, A., Ashique, R.H., ul Haq, M.A., Shihavuddin, A.S.M. and Jadin, M.S., 2023. Feasibility analysis of floating photovoltaic power plant in Bangladesh: A case study in Hatirjheel Lake, Dhaka. Sustainable energy technologies and assessments, 55, p.102994.

[13] Ateş, A.M., 2022. Unlocking the floating photovoltaic potential of Türkiye's hydroelectric power plants. Renewable Energy, 199, pp.1495-1509.

[14] Temiz, M. and Dincer, I., 2022. Design and analysis of a floating photovoltaic based energy system with underground energy storage options for remote communities. Journal of Energy Storage, 55, p.105733.

[15] Peng, L., Liu, B., Zheng, S., Chen, X., Zhong, Q. and Chai, X., 2023. A new dynamic 2D fusion model and output characteristic analysis of floating photovoltaic modules considering motion and environmental factors. Energy Conversion and Management, 294, p.117588.

[16] Mumtaz, A., Abbas Kazmi, S.A., Altamimi, A., Khan, Z.A. and Alyami, S., 2024. Multi-dimensional potential assessment of grid-connected mega-scale floating PV power plants across heterogeneous climatic zones. Frontiers in Energy Research, 12, p.1404777.

[17] Chirwa, D., Goyal, R. and Mulenga, E., 2023. Floating solar photovoltaic (FSPV) potential in Zambia: Case studies on six hydropower power plant reservoirs. Renewable Energy Focus, 44, pp.344-356.

[18] Alsunousi, M. and Kayabasi, E., 2024. Techno-economic assessment of a floating photovoltaic power plant assisted methanol production by hydrogenation of CO_2 captured from Zawiya oil refinery. International Journal of Hydrogen Energy, 57, pp.589-600.

[19] Moravej, M., Noghrehabadi, A., Esmaeilinasab, A.L.I. and Khajehpour, E., 2020. The effect of SiO_2 nanoparticle on the performance of photovoltaic thermal system: Experimental and Theoretical approach. Journal of Heat and Mass Transfer Research, 7(1), pp.11-24.

[20] Balal, A., Sheikhzadeh, G.A. and Fattahi, A., 2024. Experimental evaluation of the hybrid-bifacial cooling of a PV panel in arid weather using channel heat exchanger and impingement flow nozzles. Journal of Heat and Mass Transfer Research, 11(2), pp.195-210.

[21] Sardoii, E.R., Rostami, N., Sigaroudi, S.K. and Taheri, S., 2012. Calibration of loss estimation methods in HEC-HMS for simulation of surface runoff (Case Study: Amirkabir Dam Watershed, Iran). Adv. Environ. Biol, 6(1), pp.343-348.

[22] Losgedaragh, S.Z. and Rahimzadegan, M., 2018. Evaluation of SEBS, SEBAL, and METRIC models in estimation of the evaporation from the freshwater lakes (Case study: Amirkabir dam, Iran). Journal of hydrology, 561, pp.523-531.

[23] Kalogirou, S.A., 2023. Solar energy engineering: processes and systems. Elsevier.

[24] Gow, J.A. and Manning, C.D., 1999. Development of a photovoltaic array model for use in power-electronics simulation studies. IEE Proceedings-Electric Power Applications, 146(2), pp.193-200.

[25] Badi, N., Khasim, S., Al-Ghamdi, S.A., Alatawi, A.S. and Ignatiev, A., 2021. Accurate modeling and simulation of solar photovoltaic panels with simulink-MATLAB. Journal of Computational Electronics, 20, pp.974-983.

[26] Anani, N. and Ibrahim, H., 2020. Adjusting the single-diode model parameters of a photovoltaic module with irradiance and temperature. Energies, 13(12), p.3226.

[27] Suh, J., Jang, Y. and Choi, Y., 2019. Comparison of electric power output observed and estimated from floating photovoltaic systems: A case study on the hapcheon dam, Korea. Sustainability, 12(1), p.276.

[28] Triyana, K., Yasuda, T., Fujita, K. and Tsutsui, T., 2004. Effects of different materials used for internal floating electrode on the photovoltaic properties of tandem type organic solar cell. Japanese journal of applied physics, 43(4S), p.2352.

[29] Kumar, N.M., Subramaniam, U., Mathew, M., Ajitha, A. and Almakhles, D.J., 2020. Exergy analysis of thin-film solar PV module in ground-mount, floating and submerged installation methods. Case Studies in Thermal Engineering, 21, p.100686.

[30] Jariso, M., Khan, B., Tesfaye, D. and Singh, J., 2017, April. Modeling and designing of stand-alone photovoltaic system: CaseStudy: Addis Boder health center south west Ethiopia. In 2017 International conference of Electronics, Communication and Aerospace Technology (ICECA) (Vol. 1, pp. 168-173). IEEE.

[31] Taye, B.Z., Nebey, A.H. and Workineh, T.G., 2020. Design of floating solar PV system for typical household on Debre Mariam Island. Cogent Engineering, 7(1), p.1829275.

[32] Muslim, H.N., Solar tilt angle optimization of PV systems for different case studies. EAI Endorsed Transactions on Energy Web, 2019. 6(23): p. e7-e7.

[33] Liu, L., Sun, Q., Li, H., Yin, H., Ren, X. and Wennersten, R., 2019. Evaluating the benefits of integrating floating photovoltaic and pumped storage power system. Energy Conversion and Management, 194, pp.173-185.

[34] Norton, B., Eames, P.C. and Lo, S.N., 1998. Full-energy-chain analysis of greenhouse gas emissions for solar thermal electric power generation systems. Renewable energy, 15(1-4), pp.131-136.